ADVANCES IN ATMOSPHERIC SCIENCES
大气科学进展

EARLY ONLINE RELEASE

The DOI for this manuscript is doi: 10.1007/s00376-015-4209-5.

Do European Blocking Events Precede North Atlantic Oscillation Events?

YAO Yao and LUO Dehai*

Key Laboratory of Regional Climate-Environment for Temperate East Asia (RCE-TEA), Institute of Atmospheric Physics, Chinese Academy of Science, Beijing 100029

(Received 19 September 2014; revised 20 January 2015; accepted 2 February 2015)

ABSTRACT

Using a two-dimensional blocking index, the cause and effect relationship between European blocking (EB) events and North Atlantic Oscillation (NAO) events is investigated. It is shown that the EB event frequency is enhanced over Northern (Southern) Europe for negative (positive) phases of the NAO. Enhanced EB events over Northern Europe precede the establishment of negative phase NAO (NAO^-) events, while the enhanced frequency of EB events over Southern Europe lags positive phase NAO (NAO^+) events.

The physical explanation for why enhanced EB events over Northern (Southern) Europe lead (lag) NAO^- (NAO^+) events is also provided. It is found that the lead--lag relationship between EB events in different regions and the phase of NAO events can be explained in terms of the different latitudinal distribution of zonal wind associated with the different phases of NAO events. For NAO^+ events, the self-maintained eastward displacement of intensified midlatitude positive height anomalies owing to the intensified zonal wind can enhance the frequency of EB events over

*Corresponding author: LUO Dehai
Email: ldh@mail.iap.ac.cn

Southern Europe, thus supporting a standpoint that EB events over Southern Europe lag NAO^+ events. Over Northern Europe, EB events lead NAO^- events because NAO^- events arise from the self-maintained westward migration of intensified blocking anticyclones due to the weakened zonal wind in higher latitudes.

Key words: European blocking, North Atlantic Oscillation, mutual relationship

1. Introduction

The North Atlantic Oscillation (NAO) is an important low frequency mode of climate variability in the Northern Hemisphere (NH), identified as a north--south dipole pattern confined to the Atlantic basin (Hurrell, 1995). The basic dynamics of NAO events has been an important research direction (Feldstein, 2003; Luo et al., 2007a, 2007b; Luo and Cha, 2012) because of its importance in climate changes in the NH (Scaife et al., 2008; Sillmann et al., 2011).

Many studies have demonstrated that negative (positive) phase NAO events, hereafter referred to as NAO^- (NAO^+) events, arise from the cyclonic (anticyclonic) wave breaking of synoptic-scale waves (Benedict et al., 2004; Franzke et al., 2004; Rivière and Orlanski, 2007; Woollings et al., 2008; Strong and Magnusdottir, 2008), which are also suggested to correspond to the presence (absence) of blocked days over the North Atlantic (Luo et al., 2007a; Woollings et al., 2008). However, based upon a nonlinear multi-scale interaction model of NAO events developed by Luo et al. (2007a, 2007b), Luo et al. (2008) suggested that synoptic wave breaking is not a cause of NAO onset, but instead is a concomitant result of the eddy-induced intensified NAO pattern. Other studies have established links between the phase of the NAO and blocking activity (Shabbar et al., 2001; Luo, 2005; Scherrer et al., 2006; Croci-Maspoli et al., 2007; Luo et al., 2007a, 2014). Among these studies, an interesting result is that the negative (positive) phase of the NAO corresponds to an enhanced

blocking frequency over Greenland (Europe). In terms of a wave breaking index, Woollings et al. (2008) suggested that NAO^- (NAO^+) events may arise from the succession of blocked (non-blocked) days over Greenland. Feldstein (2003) and Sung et al. (2011) attributed NAO^- events to the existence of a blocking-type anomaly over Northern Europe. More recently, Davini et al. (2012b) found that the reduction of the Greenland blocking frequency leads to an eastward shift of the NAO pattern. Although these studies have revealed a close link between European blocking (EB) events and the phase of NAO events, the cause and effect relationship between EB events and NAO events remains unclear. This is a critical problem that we attempt to investigate in the present paper.

The remainder of the paper is organized as follows: In section 2, we describe the data and blocking index used in the analysis. Section 3 depicts the geographical distributions of the winter-mean blocking frequency, as well as the instantaneous blocking (IB) frequencies associated with *in-situ* NAO events and transition events. We examine the cause and effect relationship between EB events and the phase of the NAO in section 4. A physical explanation of the lead–lag relationship between EB events and the phase of the NAO is presented in section 5. A self-maintaining mechanism of the westward (eastward) migration of the NAO^- (NAO^+) dipole pattern is also proposed in this section. Finally, the key conclusions are summarized, and further discussion is provided, in section 6.

2. Data and methodology

2. 1 *Data description and definition of an NAO event*

This study uses the daily multi-level geopotential height and wind fields from the National Centers for Environmental Prediction/National Center for Atmospheric Research (NCEP/NCAR) reanalysis at a horizontal resolution of $2.5° \times 2.5°$ from 1950 to 2011. In this paper, we focus on

winter, defined as the time interval from November to March. The daily anomaly, for which the seasonal cycle is removed, is defined as the deviation of the daily field from its climatological time mean. An NAO^+ (NAO^-) event is defined if the normalized daily NAO index is greater (less) than or equal to +1.0 (−1.0) standard deviation persisting for at least three consecutive days. The daily NAO index, defined as the Rotated Empirical Orthogonal Function (REOF) of daily geopotential height fields at 500 hPa, is available from the National Oceanic and Atmospheric Administration/Climate Prediction Center (Kalnay et al., 1996).

Following Luo et al. (2012a), NAO events are categorized into two types: *in-situ* (individual) NAO events and transition events. The *in-situ* NAO events are defined as those events with only one phase, either NAO^+ or NAO^-. The transition events are defined as those events of one phase followed by the opposite phase, and must include both NAO^+ and NAO^- events. A detailed definition of NAO transition events can be found in Luo et al. (2012a).

Based on the definitions of these events, we detect 99 *in-situ* NAO^- events and 97 *in-situ* NAO^+ events, as well as 38 NAO^+ to NAO^- and 30 NAO^- to NAO^+ transition events in winter during the period from 1950 to 2011. In this paper, lag(0) represents the day with maximum amplitude during the NAO (NAO^+ and NAO^-) life cycle. For transition NAO events, lag(0) represents the day with maximum amplitude during the NAO^+ of NAO^+ to NAO^- transition events and the NAO^- of NAO^- to NAO^+ transition events, respectively.

2.2 *Two-dimensional blocking index*

In recent years, many two-dimensional (2D) blocking indices have been proposed to identify the spatial and temporal variations of blocking events (Barriopedro et al., 2006, 2010; Diao et al., 2006; Scherrer et al., 2006; Davini et al., 2012a, 2012b) based upon the extension of one-dimensional

blocking indices (Lejenäs and Okland, 1983; Tibaldi and Molteni, 1990; Pelly and Hoskins, 2003). The recent 2D blocking index developed by Davini et al. (2012a) has the advantage of differentiating high-latitude and low-latitude events of blocking flows in the Euro-Atlantic sector compared to other 2D indices (Diao et al., 2006). Thus, it is appropriate to use the 2D blocking index of Davini et al. (2012a, 2012b) to perform our investigation because our focus is on the spatiotemporal variation of Euro-Atlantic blocking events. To detect IB events in the Euro-Atlantic region, analogous to Davini et al. (2012a) we define the meridional gradient reversal of the 500-hPa geopotential height at each grid point as

$$\mathrm{GHGS}(\lambda_0,\phi_0)=\frac{Z(\lambda_0,\phi_0)-Z(\lambda_0,\phi_S)}{\phi_0-\phi_S}, \tag{1}$$

$$\mathrm{GHGN}(\lambda_0,\phi_0)=\frac{Z(\lambda_0,\phi_\mathrm{N})-Z(\lambda_0,\phi_0)}{\phi_\mathrm{N}-\phi_0}, \tag{2}$$

$$\mathrm{GHGS}(\lambda_0,\phi_0)>0 \qquad \mathrm{GHGN}(\lambda_0,\phi_0)<-10, \tag{3}$$

$$\mathrm{GHGS}_2(\lambda_0,\phi_0)=\frac{Z_{500}(\lambda_0,\phi_\mathrm{S})-Z_{500}(\lambda_0,\phi_\mathrm{S}-15)}{15}<-5, \tag{4}$$

where $Z(\lambda_0,\phi_0)$ is the daily 500-hPa geopotential height at the grid point (λ_0, ϕ_0), λ_0 (ϕ_0) is the longitude (latitude) ranging from 0° to 360°W (30°N to 75°N), $\phi_N=\phi_0+15$, and $\phi_S=\phi_0-15$ (Davini et al., 2012a, 2012b). GHGN and GHGS represent the geopotential height gradients (units: m per 1° of latitude) at 500 hPa over the north and south sides of (λ_0,ϕ_0).

One can identify an IB event if conditions (1--4) are satisfied. Here, very low-latitude blocking events such as subtropical ridges in the Atlantic basin are excluded through constraint (4). According to the definition of a blocking event (Davini et al., 2012a, 2012b), an IB event satisfies conditions (1--4). However, a blocking event is a continuous process of an IB event persisting for at least 5 days at a given grid point and has at least a large spatial scale [such as 5°(lat) × 10°(lon), as described in

Davini et al. (2012a)]. Because the frequency of IB events exhibits a striking resemblance to that of blocking events, the IB frequency in the Euro-Atlantic sector is only calculated and used as a measure of the blocking occurrence in this paper. The sensitivity of this 2D blocking index defined in Eq. (1) to different data is examined in Davini et al. (2012a).

3. Geographical distribution of Euro-Atlantic blocking events and its link with the phase of NAO events

To understand the possible impact of NAO events on the spatial distribution of blocking events in the Euro-Atlantic sector, it is reasonable to use the 2D blocking index of Davini et al. (2012a, 2012b) to calculate the IB frequency. Figure 1 shows the geographical distributions of the winter mean IB frequency as well as the spatial distributions of the composite IB frequencies associated with *in-situ* NAO and transition events during 1950–2011. Here, the winter mean IB frequency reflects the IB climatology in winter, which is measured as the percentage of blocked days with respect to the total days of winter during 1950--2011. The calculation is applied during the life cycle of an NAO event [from lag(−10) to lag(+10) for *in-situ* NAO events, but from lag(−10) to lag(+5) and lag(+5) to lag(+25) for NAO transition events]. It is evident that there are two frequency centers of blocking events in the Euro-Atlantic sector: Greenland and Central Europe (Fig. 1a). However, the occurrence region of Euro-Atlantic blocking events is modulated by the variation of the NAO phase. For the positive phase of *in-situ* NAO events, the higher IB frequency is concentrated in one region from the central-eastern Atlantic to Southern Europe (Fig. 1b), while the IB frequency for the negative phase has two maximum regions: Greenland and Northern Europe (Fig. 1c). Thus, the action center of Euro-Atlantic blocking events is affected by the phase of *in-situ* NAO events.

If an NAO event undergoes a transition from one phase to another, the geographical distribution of the IB frequency can exhibit a marked change from a southwest--northeast (southeast--northwest) pattern distribution to another in the southeast--northwest (southwest--northeast) direction (Figs. 1e--g). The results are evidently different from the previous results of Scherrer et al. (2006) and Croci-Maspoli et al. (2007), who only noted that the blocking frequency is enhanced (reduced) over Europe for positive (negative) phases. However, here we detect a new result that there is an enhanced blocking frequency over Southern (Northern) Europe for positive (negative) phases. Thus, the phase of NAO events seems to play a crucial role in controlling the spatial distribution of EB events.

As can be seen from the data in Table 1, the numbers of transition NAO events are smaller than those of *in-situ* NAO events. Statistical analysis indicates that the total number of days of *in-situ* NAO events accounts for about 60% of the total number of NAO event days. Actually, transition NAO events are a combination of two phases of *in-situ* NAO events. The impact of NAO^+ (NAO^-) episodes of NAO^+ to NAO^- transition events on IB frequency is similar to *in-situ* NAO^+ (NAO^-) events, and vice versa for NAO^- to NAO^+ transition events. The regime transition of NAO events plays an important role in the interannual variability of the NAO (Luo et al., 2012a, 2012b), but this is beyond the scope of the current paper. Thus, in this study, we focus only on analyzing *in-situ* NAO events.

4. Cause and effect relationship between EB events and NAO events

4. 1 *IB frequency indices and their relationship with NAO events*

To describe the longitudinal and latitudinal variations of Euro-Atlantic blocking events, the regions (60 °--77.5 °N, 10 °W--30 °E) and (35 °--50 °N, 10 °W--30 °E) are defined as Northern Europe and Southern Europe, respectively. Correspondingly, the regions (60 °--77.5 °N, 60 °--10 °W) and

(35°--50°N, 60°--10°W) are defined as the high-latitude North Atlantic and low-latitude North Atlantic, respectively. By averaging the IB frequencies in each grid within these four regions, we can construct time series of the winter IB frequency index in each region during 1950--2011 and show the normalized time series of the winter IB frequencies in the four regions in Fig. 2. The IB frequency index in each region is defined to be high (low) if the normalized index of the IB frequency is greater (less) than or equal to +1.0 (−1.0) the standard deviation. Based on the number of winters that correspond to high and low IB frequencies, the numbers of *in-situ* NAO^+, *in-situ* NAO^-, NAO^+ to NAO^- transition events, and NAO^+ to NAO^- transition events can be calculated, the results of which are shown in Table 1. It can be seen that *in-situ* NAO^- (NAO^+) events are more (less) frequent for high IB frequency winters compared to low IB frequency winters over Northern Europe. In Southern Europe, the frequency of *in-situ* NAO^- (NAO^+) events is higher for low (high) IB frequency winters compared to high (low) IB frequency winters. This suggests that frequent *in-situ* NAO^- (NAO^+) events correspond to high (low) IB frequency over Northern Europe or low (high) IB frequency over Southern Europe. Similarly, the high frequency of *in-situ* NAO^- (NAO^+) events is seen for high (low) IB frequency winters in the high-latitude North Atlantic. In contrast, the *in-situ* NAO^- (NAO^+) events have a high frequency for low (high) IB frequency winters in the low-latitude North Atlantic. Thus, the difference in the blocking event frequency in different regions is closely related to the phase of *in-situ* NAO events.

4.2 *Empirical Orthogonal Function patterns of the monthly mean geopotential height anomalies for high IB frequency winters in different regions*

In this subsection, Empirical Orthogonal Function (EOF) analysis is used to identify the leading modes of high IB index winters for different regions.

For high IB frequency winters in Northern Europe, Southern Europe, the high-latitude North Atlantic, and low-latitude North Atlantic, we show the leading and second EOF components of monthly mean 500-hPa geopotential height fields and their corresponding principal component time series in Figs. 3 and 4, respectively. It is clear that when the IB frequency in Northern Europe is higher (Fig. 3a), the leading EOF (EOF1), which explains 26.3% of the total variance, shows a northwest--southeast oriented NAO^- pattern, while the second EOF (EOF2), which explains 23.7% of the total variance, shows a Scandinavian blocking pattern (Cassou et al., 2004). However, the EOF1 and EOF2 correspond to NAO^+ and negative phase Eastern-Atlantic (EA^-) patterns (Moore and Renfrew, 2012) respectively for low IB frequency winters (less than or equal to −1.0 standard deviation for the IB frequency index) in Northern Europe (not shown). For a high IB frequency in Southern Europe, the EOF1 (EOF2) exhibits an NAO^+ (EA^-) pattern (Fig. 3b). The EOF1 and EOF2 for the low IB frequency over Southern Europe are similar to those for high IB frequency over Northern Europe (not shown). For a high IB frequency in the high-latitude North Atlantic, the EOF1 and EOF2 describe the northwest–southeast and northeast--southwest oriented NAO^- patterns (Fig. 4a), in which the EOF2 pattern seems to have a more evident eastward migration. However, for low IB frequency in the high-latitude North Atlantic, the EOF1 and EOF2 exhibit the NAO^+ and EA^- patterns (not shown). This result is also seen for high IB frequency in the low-latitude North Atlantic (Fig. 4b). When the IB frequency is low in the low-latitude North Atlantic, the EOF1 and EOF2 describe the northwest--southeast oriented NAO^- pattern and Scandanavian blocking pattern, respectively (not shown), which is also detected for high IB frequency over Northern Europe and low IB frequency over Southern Europe. Thus, this suggests a strong linkage between changes in blocking frequencies in different regions and variations of monthly mean EOF patterns. Therefore,

the connection between the phase of the NAO and the variation of blocking frequency can be seen in terms of the EOF analysis of the monthly mean height field data. This motivates us to further examine the lead–lag relationship between EB and NAO events from the daily data in the next subsection.

4.3 *Lead--lag relationship between the composite daily NAO and IB frequency indices in different regions*

To further reveal the lead–lag relationship between EB events and NAO events, we construct composites of the daily NAO indices and IB frequencies in different regions (Fig. 5). It can be seen that the daily NAO^- index has a 2-day negative correlation delay of −0.89 with the IB frequency over Northern Europe (Fig. 5a) from lag(−10) to lag(+10), which is statistically significant at the 99.9% confidence level (Glahn, 1968). Further analysis indicates that 21 (80.8%) of 26 *in-situ* NAO^- events are lagged by EB events. Thus, EB events lead the onset of NAO^- events. This result was also noted by Schwierz et al. (2004) and Sung et al. (2011). Sung et al. (2011) found that blocking ridges over Northern Europe contribute to the growth of NAO^- events through a low-frequency eddy interaction. Nevertheless, the IB frequency over Southern Europe tends to have a 3-day positive correlation delay of 0.81 with the composite daily NAO^+ index (Fig. 5b). This correlation is significant at the 99.9% confidence level. In addition, 29 (87.9%) of 33 *in-situ* NAO^+ events are found to precede EB events. Hence, EB events over Southern Europe lag NAO^+ Events. Thus, it seems reasonable to attribute an enhanced EB event frequency over Southern Europe to the genesis of NAO^+ events. However, a noticeably different characteristic is found in the high-latitude North Atlantic and low-latitude North Atlantic, where the daily NAO index and IB frequency exhibit an in-phase correlation (Figs. 5c and d). The correlation coefficient is particularly high for the high IB frequencies over the high-latitude

North Atlantic and low-latitude North Atlantic. For example, during the NAO^- (NAO^+) life cycle the coefficient of their negative (positive) correlation is −0.94 (0.92). As a result, the relationship between the phase of the NAO and blocking events is different between the Atlantic basin and continental Europe. Thus, we can conclude from the results presented here that EB events over Northern (Southern) Europe may lead (lag) the genesis of NAO^- (NAO^+) events. The results are new, although the result of NAO^- events lagging blocking events over Northern Europe was also noted by Sung et al. (2011).

5. Physical mechanism of the lead–lag relationship between EB events and NAO events.

5.1 *Role of initial large-scale anomalies in the growth of the two phases of the NAO*

To reveal the physical mechanism of the lead (lag) correlation between EB events and NAO^- (NAO^+) events, we show the composite maps of daily 500-hPa geopotential height anomalies of *in-situ* NAO^- (NAO^+) events for high IB frequency over Northern (Southern) Europe from lag(−6) to lag(4) (during the life cycle of the NAO) in Fig. 6. As can be seen from Fig. 6a, an anticyclonic anomaly appears over Northern Europe at lag(−6). The anticyclonic anomaly grows owing to the high-frequency eddy forcing (Luo et al., 2007a) and the cyclonic wave breaking (Benedict et al., 2004; Franzke et al., 2004; Rivière and Orlanski, 2007; Woollings et al., 2008). The amplified anticyclonic anomaly over Northern Europe undergoes a westward migration and extends toward the western North Atlantic, and then establishes an NAO^- dipole pattern [at lag(0)] through combining with an amplified cyclonic anomaly to its south. Thus, blocking ridges over Northern Europe prior to the negative phase of the NAO may be considered as a precursor to NAO^- events. Feldstein (2003) attributed the maintenance of the NAO anomaly to high-frequency eddy forcing, but the NAO decay to Ekmann dissipation; whereas, Luo et al. (2007a) suggested that the growth and decay of the NAO

anomaly is due to positive synoptic-scale eddy forcing and the reversal of its sign. Sung et al. (2011) noted that NAO^- events frequently accompany blocking ridges over the Barents Sea and are primarily forced by the strong positive low-frequency eddy forcing related to blocking ridges over Northern Europe.

In Fig. 6b we can see that a cyclonic anomaly appears over the western North Atlantic at lag(−6). Thus, the cyclonic anomaly in the western North Atlantic is a precondition of the onset of NAO^+ events. The initial growth of the cyclonic anomaly results from the negative low-frequency eddy forcing over the western North Atlantic and Greenland (Sung et al., 2011). However, its subsequent growth (decay) during the entire life cycle is more likely to be due to high-frequency eddy forcing (Luo et al., 2007a) or due to the presence (absence) of the anticyclonic wave breaking of synoptic-scale eddies (Benedict et al., 2004; Woollings et al., 2008). Moreover, the anticyclonic anomaly in the low-latitude North Atlantic intensifies with the growth of the cyclonic anomaly in the high-latitude North Atlantic. This process will cause the establishment of an NAO^+ event. During the growing process, the NAO^+ dipole pattern can undergo eastward migration and extension toward continental Europe, which is consistent with the result of Luo and Cha (2012). Because the anticyclonic anomaly of the NAO^+ dipole pattern occupies a broader region in the midlatitudes, it can even extend into the Urals region during the mature stage of an NAO^+ event from lag(−1) to lag(+1) (not shown). In this case, it is inevitable that we see an enhanced frequency of EB events (in the form of an anticyclonic anomaly) over Southern Europe during NAO^+ growth. Consequently, it is concluded that EB events over Southern Europe lag NAO^+ events.

It should be pointed out that EB events in Northern Europe in fact correspond to an anticyclonic anomaly over the region. When an EB event undergoes westward migration and extends toward the

North Atlantic, it becomes an NAO^- event. The observational study of Sung et al. (2011) indicates that most NAO^- events result from the westward migration of amplifying Northern European anticyclones. Thus, to some extent, the anticyclonic anomaly over Northern Europe (the North Atlantic) is the flow reflection of an EB (NAO^-) event.

5.2 *Longitudinal migration of geopotential height anomalies in different latitudinal bands during the life cycle of the NAO for its two phases*

To reflect the zonal migration of the geopotential height anomalies (especially positive anomalies) for different phases of the NAO, Hovmöller diagrams of the composite daily geopotential height anomalies averaged over 60°–77.5°N (35°–50°N) for the negative (positive) phase are shown in Fig. 7 for high IB frequencies over Northern Europe, Southern Europe, the high-latitude North Atlantic, and the low-latitude North Atlantic. It is clear that for the negative phase of the NAO the positive anomaly over Northern Europe undergoes a noticeable westward shift after lag(−6) (Fig. 7a), and continues its westward migration until lag(+6). The positive anomaly tends to reach its strongest amplitude near 40°W at lag(0). Such a westward migration is also seen in the high-latitude North Atlantic (Fig. 7c), where only the distinct westward migration is detected before lag(0), and the strongest amplitude occurs at lag(0) and locates near 40°W. Although the westward shift of positive anomalies is somewhat weaker in the high-latitude North Atlantic than in Southern Europe, it is concluded that the genesis of NAO^- events results from the westward migration of amplified anticyclonic anomalies that initiate over Northern Europe.

On the other hand, for the positive phase of the NAO, it is found that the positive anomaly undergoes an eastward migration not only in the low-latitude North Atlantic (Fig. 7d), but also in Southern Europe (Fig. 7b). Such an eastward shift persists during the entire lifespan of an NAO^+

event. In particular, the amplified positive anomaly can extend more eastward into inland continental Europe, leading to an enhanced EB event frequency over Southern Europe. Thus, it is concluded that EB events over Southern Europe lag NAO^+ events. The result that EB events over Northern (Southern) Europe lead (lag) NAO^- (NAO^+) events can be interpreted in terms of a self-maintaining mechanism of the longitudinal migration of the NAO dipole pattern, as proposed in the next subsection.

5.3 *Self-maintaining mechanism of the westward (eastward) migration of NAO^- (NAO^+) events*

To understand the physical cause of the westward (eastward) migration of positive anomalies associated with NAO^- (NAO^+) events, it seems reasonable to show the meridional profile of the time-mean zonal winds averaged in the Atlantic basin (60°--10°W) and continental Europe (10°W--30°E) during the entire lifespan of NAO events (Fig. 8). It is interesting to see that the zonal wind over Northern Europe (50°--70°N) is relatively weak for the negative phase of the NAO relative to the positive phase (Fig. 8b). The amplified positive anomaly inevitably undergoes a westward shift once the positive anomaly that initiates over Northern Europe intensifies because of the strong eddy forcing. Because of the strengthening (weakening) of zonal wind in the low-latitude, 25°--40°N (high-latitude, 45°--65°N) Atlantic basin associated with the growing NAO^- anomaly (Fig. 8a), the weak zonal wind in the high-latitude North Atlantic tends to render the westward shift of the NAO^- dipole pattern. According to Jung et al. (2003), the strength of the mean zonal wind is a major cause of the zonal shift of the NAO dipole mode. Our result also holds if the basic mean zonal wind [defined as the zonal wind prior to NAO onset (Yao and Luo, 2014)] is used (not shown). However, Luo et al. (2010) found from both observed and theoretical aspects that the zonal shift of the NAO pattern is dominated by the meridional variation of the Atlantic jet associated with the NAO phase

due to the different phase speed. This is a possible mechanism that can be used here to provide an explanation for the results of the present study.

For the positive phase of the NAO, the zonal wind intensifies and shifts northward due to the feedback of the growing NAO^+ pattern, such that the zonal wind significantly intensifies in the midlatitudes centered at 50 °N (Fig. 8a). This result has been theoretically noted by Luo et al. (2007b; 2010). The strengthening of the zonal wind in the low-latitude (0 °--20 °N) North Atlantic can favor the eastward migration of the anticyclonic anomaly of the NAO^+ dipole pattern and its further extension into Southern Europe. This leads to an enhanced frequency of EB events over Southern Europe. Hence, it is natural that EB events over Southern Europe lag NAO^+ events.

The theoretical results of Luo et al. (2007b) based on weakly nonlinear multi-scale interaction model of NAO events have demonstrated that the strengthening (weakening) of zonal wind in the relatively low (high) latitudes of the Atlantic basin is a spontaneous consequence of NAO^- genesis. The reason is that the zonal wind is intensified (weakened) in the middle--high latitudes for the positive (negative) phase of the NAO pattern due to the presence of the intensified NAO^- (NAO^+) anomaly (Luo et al. 2007b). The weakening (strengthening) of zonal wind in the mid–high latitudes favors the westward (eastward) migration of the NAO^- (NAO^+) anomaly (Luo et al., 2010). Such a process is the so-called “self-maintaining” mechanism.

6. Conclusions and discussion

This paper examines the cause and effect relationship between EB events and the phase of the NAO. It is found that the frequency of EB events is enhanced over Northern (Southern) Europe for the negative (positive) phase of the NAO. This is a new result, different from previous findings reported by Scherrer et al. (2006), Woollings et al. (2008) and Davini et al. (2012b), who only noted

an enhanced frequency of EB events for the positive phase of the NAO. Our observational analysis shows that EB events over Northern (Southern) Europe lead (lag) NAO^- (NAO^+) events. To some extent, the results derived from this study are a complement to the previous studies of Sung et al. (2011). They found that blocking ridges over Northern Europe frequently precede negative NAO events and suggested that the low-frequency eddy forcing associated with the blocking ridges contribute positively to the initial growth of negative NAO events. However, in this paper we further find that NAO^+ events precede enhanced EB events over Southern Europe. This is a new result, not reported previously.

A self-maintaining mechanism of the westward (eastward) migration of NAO^- (NAO^+) events is proposed to explain why EB events over Northern (Southern) Europe lead (lag) NAO^- (NAO^+) events, based on the theoretical studies of Luo et al. (2007b, 2010). This mechanism suggests that the westward (eastward) migration of NAO^- (NAO^+) events can be attributed to the weakening (strengthening) of the zonal wind in the middle-–high latitudes owing to the feedback of the NAO^- (NAO^+) dipole pattern (Luo et al., 2007b). Thus, it is concluded that EB events over Northern (Southern) Europe leading (lagging) NAO^- (NAO^+) events during the NAO^- (NAO^+) life cycle is a self-maintaining phenomenon.

Although the focus of the present paper is not on the physical mechanism of NAO genesis, the physical mechanism of the onset of NAO events can be better explained in terms of the nonlinear multi-scale interaction model of NAO events (Luo et al., 2007a, 2007b). With the weakening (intensifying) of zonal winds in middle-–high latitudes during the growth of an NAO^- (NAO^+) event, the amplified anticyclonic anomaly of the NAO^- (NAO^+) dipole pattern undergoes a marked westward (eastward) migration away from the source region. Such an opposite zonal migration

between the NAO^- and NAO^+ dipole patterns implies that there is a lead (lag) relationship between EB events over Northern (Southern) Europe and NAO^- (NAO^+) events because the anticyclonic anomaly is often identified as a blocking event.

However, it must be pointed out that the blocking latitude location in continental Europe is significantly different between the positive and negative phases of the NAO. Whether or not the different latitude location of blocking events over Europe can exert a significant influence on extreme weather events is not addressed in the present paper, but further understanding of this problem is needed.

Acknowledgements. The authors acknowledge the support from the National Natural Science Foundation of China (Grant Nos. 41375067 and 41430533) and we thank the two anonymous reviewers for their constructive comments for improving this paper.

REFERENCES

Barriopedro, D., R. García-Herrera, A. R. Lupo, and E. Hernández, 2006: A climatology of Northern Hemisphere blocking. *J. Climate*, **19**, 1042--1063, doi: 10.1175/JCLI3678.1.

Barriopedro, D., R. García-Herrera, and R. M. Trigo, 2010: Application of blocking diagnosis methods to General Circulation Models. Part I: A novel detection scheme. *Climate Dyn.*, **35**, 1373--1391, doi: 10.1007/s00382-010-0767-5.

Benedict J. J., S. Lee, and S. B. Feldstein, 2004: Synoptic view of the North Atlantic Oscillation. *J. Atmos. Sci.*, **61**, 121--144.

Cassou, C., L. Terray, J. W. Hurrell, and C. Deser, 2004: North Atlantic winter climate regimes: Spatial asymmetry, stationarity with time, and oceanic forcing. *J. Climate*, **17**, 1055--1068.

Croci-Maspoli, M., C. Schwierz, and H. C. Davies, 2007: Atmospheric blocking: Space--time links to the NAO and PNA. *Climate Dyn*., **29**, 713--725.

Davini, P., C. Cagnazzo, S. Gualdi, and A. Navarra, 2012a: Bidimensional diagnostics, variability, and trends of Northern Hemisphere blocking. *J. Climate*, **25**, 6496--6509.

Davini, P., C. Cagnazzo, R. Neale, and J. Tribbia, 2012b: Coupling between Greenland blocking and the North Atlantic Oscillation pattern. *Geophys. Res. Lett.*, **39**, l14701, doi: 10.1029/2012GL052315.

Diao, Y. N., J. P. Li, and D. H. Luo, 2006: A new blocking index and its application: Blocking action in the Northern Hemisphere. *J. Climate,* **19**, 4819--4839.

Feldstein, S. B., 2003: The dynamics of NAO teleconnection pattern growth and decay. *Quart. J. Roy. Meteor. Soc.*, **129**, 901--924.

Franzke, C., S. Lee, and S. B. Feldstein, 2004: Is the North Atlantic Oscillation a breaking wave? *J. Atmos. Sci*., **61**, 145--160.

Glahn, H. R., 1968: Canonical correlation and its relationship to discriminant analysis and multiple regression. *J. Atmos. Sci*., **25**, 23--31.

Hurrell, J. W., 1995: Decadal trends in the North Atlantic Oscillation: Regional temperatures and precipitation. *Science*, **269**, 676--679.

Jung, T., M. Hilmer, E. Ruprecht, S. Kleppek, S. K. Gulev, and O. Zolina, 2003: Characteristics of the recent eastward shift of interannual NAO variability. *J. Climate*, **16**, 3371--3382.

Kalnay, E., and Coauthors, 1996: The NCEP/NCAR 40-Year Reanalysis Project. *Bull. Amer. Meteor. Soc*., 77, 437–471.

Lejenäs, H., and H. Økland, 1983: Characteristics of northern hemisphere blocking as determined

from a long time series of observational data. *Tellus A*, **35A**, 350--362.

Luo, D. H., 2005: Why is the North Atlantic block more frequent and long-lived during the negative NAO phase? *Geophys. Res. Lett.*, **32**, L20804, doi: 10.1029/2005GL022927.

Luo, D. H., and J. Cha, 2012: The North Atlantic Oscillation and the North Atlantic jet variability: Precursors to NAO regimes and transitions. *J. Atmos. Sci.*, **69**, 3763--3787.

Luo, D. H., A. R. Lupo, and H. Wan, 2007a: Dynamics of eddy-driven low-frequency dipole modes. Part I: A simple model of North Atlantic Oscillations. *J. Atmos. Sci.*, **64**, 3--38.

Luo, D. H., T. T. Gong, and Y. N. Diao, 2007b: Dynamics of eddy-driven low-frequency dipole modes. Part III: Meridional displacement of westerly jet anomalies during two phases of NAO. *J. Atmos. Sci.*, **64**, 3232--3248.

Luo, D. H., T. T. Gong, and Y. N. Diao, 2008: Dynamics of eddy-driven low-frequency dipole modes. Part IV: Planetary and synoptic wave-breaking processes during the NAO life cycle. *J. Atmos. Sci.*, **65**, 737--765.

Luo, D. H., Z. H. Zhu, R. C. Ren, L. H. Zhong, and C. Z. Wang, 2010: Spatial pattern and zonal shift of the North Atlantic Oscillation. Part I: A dynamical interpretation. *J. Atmos. Sci.*, **67**, 2805--2826.

Luo, D. H., J. Cha, and S. B. Feldstein, 2012a: Weather regime transitions and the interannual variability of the North Atlantic Oscillation. Part I: A likely connection. *J. Atmos. Sci.*, **69**, 2329--2346.

Luo, D. H., J. Cha, and S. B. Feldstein, 2012b: Weather regime transitions and the interannual variability of the North Atlantic Oscillation. Part II: Dynamical processes. *J. Atmos. Sci.*, **69**, 2347--2363.

Luo, D. H., Y. Yao, and A. G. Dai, 2014: Decadal relationship between European blocking and North Atlantic oscillation during 1978--2011. Part I: Atlantic conditions. *J. Atmos. Sci.*, doi: 10.1175/JAS-D-14-0039.1.

Moore, G. W. K., and I. A. Renfrew, 2012: Cold European winters: Interplay between the NAO and the East Atlantic mode. *Atmospheric Science Letters*, **13**, 1--8.

Pelly, J. L., and B. J. Hoskins, 2003: A new perspective on blocking. *J. Atmos. Sci.*, **60**, 743--755.

Rivière, G., and I. Orlanski, 2007: Characteristics of the Atlantic storm-track eddy activity and its relation with the North Atlantic Oscillation. *J. Atmos. Sci.*, **64**, 241--266.

Scaife, A. A., C. K. Folland, L. V. Alexander, A. Moberg, and J. R. Knight, 2008: European climate extremes and the North Atlantic oscillation. *J. Climate*, **21**, 72--83, doi: 10.1175/2007JCLI1631.1.

Scherrer, S., M. Croci-Maspoli, C. Schwierz, and C. Appenzeller, 2006: Two-dimensional indices of atmospheric blocking and their statistical relationship with winter climate patterns in the Euro-Atlantic region. *International Journal of Climatology*, **26**, 233--249.

Schwierz, C., M. Croci-Maspoli, and H. C. Davies, 2004: Perspicacious indicators of atmospheric blocking. *Geophys. Res. Lett.*, **31**, L06125, doi: 10.1029/2003GL019341.

Shabbar, A., J. P. Huang, and K. Higuchi, 2001: The relationship between the wintertime North Atlantic Oscillation and blocking episodes in the North Atlantic. *International Journal of Climatology*, **21**, 355--369, doi: 10.1002/joc.612.

Sillmann, J., M. Croci-Maspoli, M. Kallache, and R. W. Katz, 2011: Extreme cold winter temperatures in Europe under the influence of North Atlantic atmospheric blocking. *J. Climate*, **24**, 5899--5913, doi: 10.1175/2011JCLI4075.1.

Sung, M. K., G. H. Lim, J. S. Kug, and S. An, 2011: A linkage between the North Atlantic Oscillation and its downstream development due to the existence of a blocking ridge. *J. Geophys. Res.*, **116**, doi: 10.1029/2010JD015006.

Strong, C., and G. Magnusdottir, 2008: Tropospheric Rossby wave breaking and the NAO/NAM. *J. Atmos. Sci*., **65**, 2861--2876.

Tibaldi, S., and F. Molteni, 1990: On the operational predictability of blocking. *Tellus A*, **42**, 343--365.

Woollings, T., B. Hoskins, M. Blackburn, and P. Berrisford, 2008: A new Rossby wave–breaking interpretation of the North Atlantic Oscillation. *J. Atmos. Sci.*, **65**, 609--626.

Yao, Y., and D. H. Luo, 2014: Relationship between zonal position of the North Atlantic Oscillation and Euro-Atlantic blocking events and its possible effect on the weather over Europe. *Science China Earth Sciences*, **57**, 2628--2636.

Table 1. Event and year numbers of *in-situ* NAO events and transition events for high and low IB frequencies over Northern Europe, Southern Europe, the high-latitude North Atlantic, and low-latitude North Atlantic. Bold numbers represent the dominant events.

	Northern Europe		Southern Europe	
	High (11 years)	Low (8 years)	High (11 years)	Low (10 years)
In situ NAO^+	9	**26**	**33**	2
In situ NAO^-	**26**	5	8	**27**
NAO^+ to NAO^-	7	4	4	7
NAO^- to NAO^+	7	3	1	6
	High-latitude North Atlantic		Low-latitude North Atlantic	
	High (12 years)	Low (9 years)	High (12 years)	Low (10 years)
In situ NAO^+	2	**30**	**29**	4
In situ NAO^-	**35**	2	9	**26**
NAO^+ to NAO^-	8	6	9	7
NAO^- to NAO^+	8	3	2	6

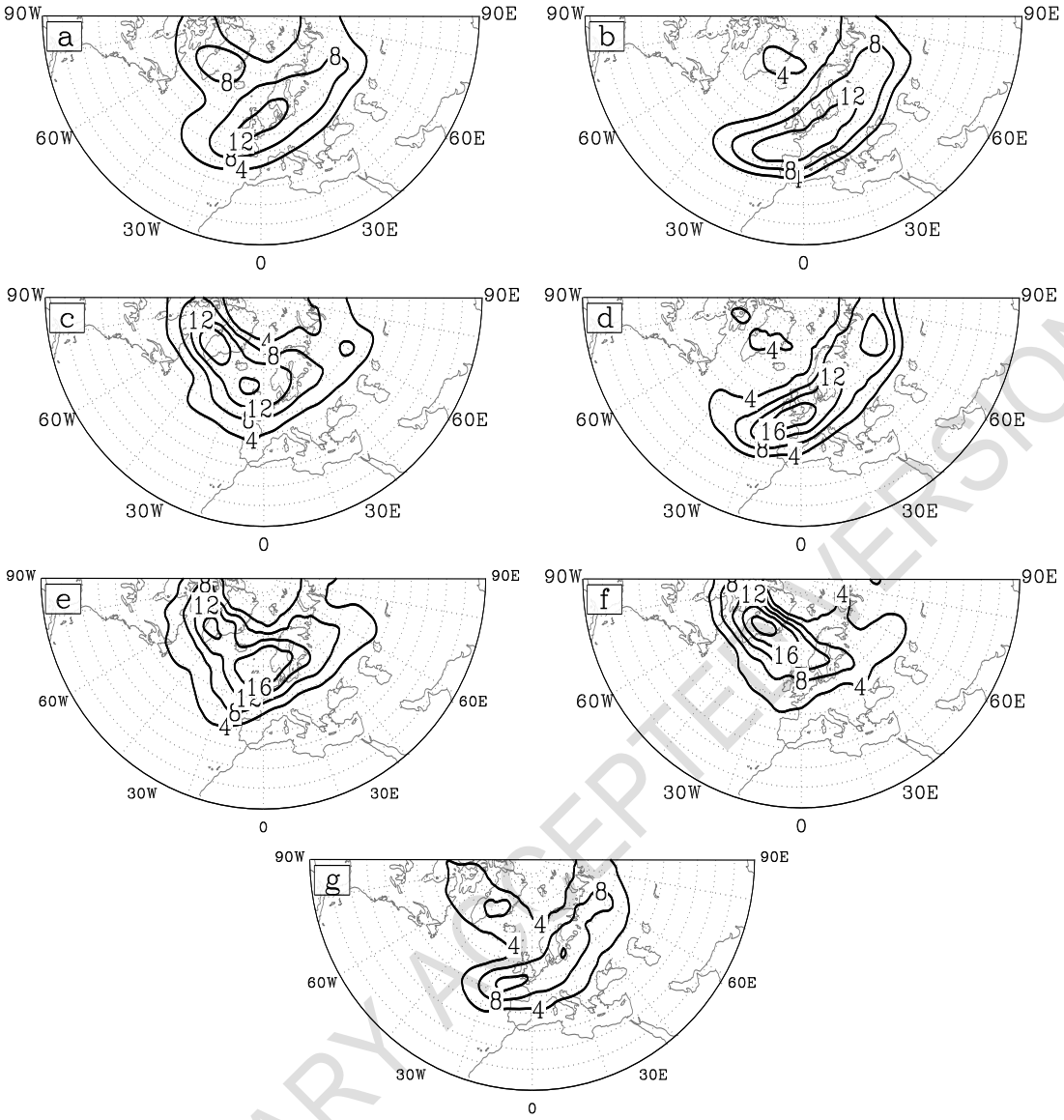

Fig. 1. Geographical distribution of instantaneous blocking frequencies for (a) total winter mean, (b) *in-situ* NAO^+ events, (c) *in-situ* NAO^- events, (d) NAO^+ to (e) NAO^- transition events, and (f) NAO^- to (g) NAO^+ transition events. The contours are representative of the percentage of blocked days with respect to total days. Contours are drawn from 4 to 20 with intervals of 4. The units are %. The latitudinal direction is plotted in 5 ° intervals starting at 20 ºN. For *in-situ* NAO events, the IB frequency is calculated during the period from lag(−10) to lag(+10), and the period for the calculation of transition events is from lag(−10) to lag(+5) and lag(+5) to lag(+20) before and after the transition, respectively.

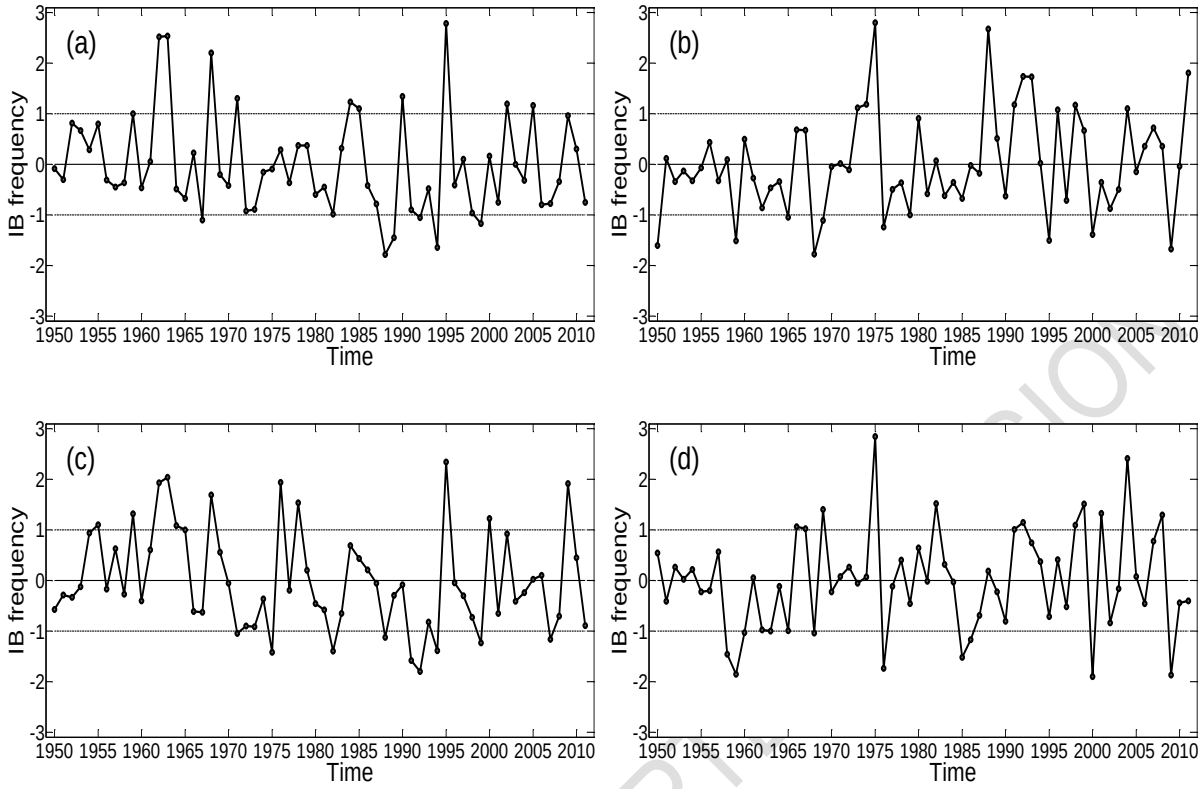

Fig. 2. Time series of normalized winter-mean IB frequencies over four regions: (a) Northern Europe, (b) Southern Europe, (c) the high-latitude North Atlantic, (d) the low-latitude North Atlantic.

(a)

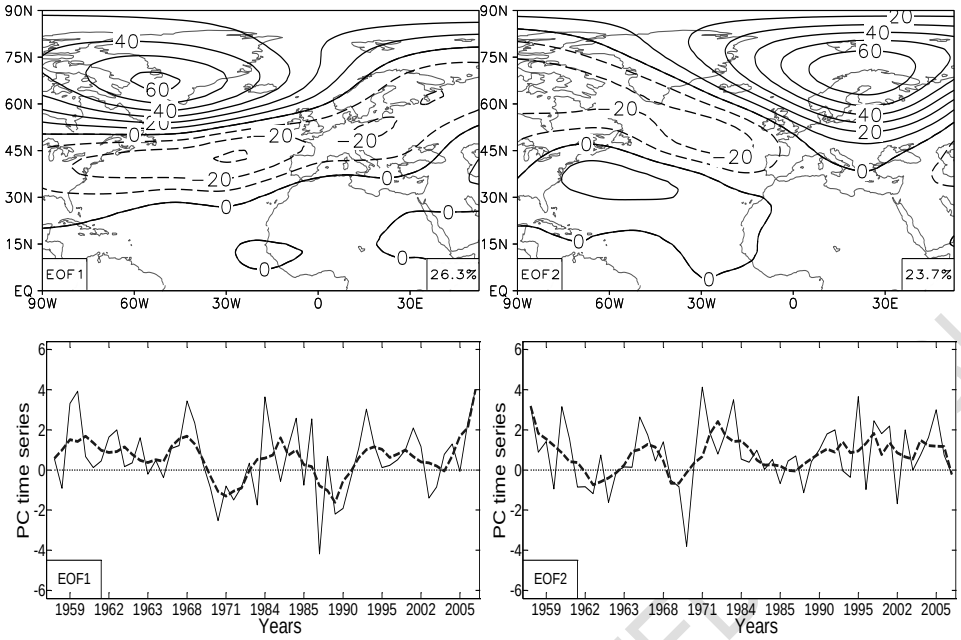

(b)

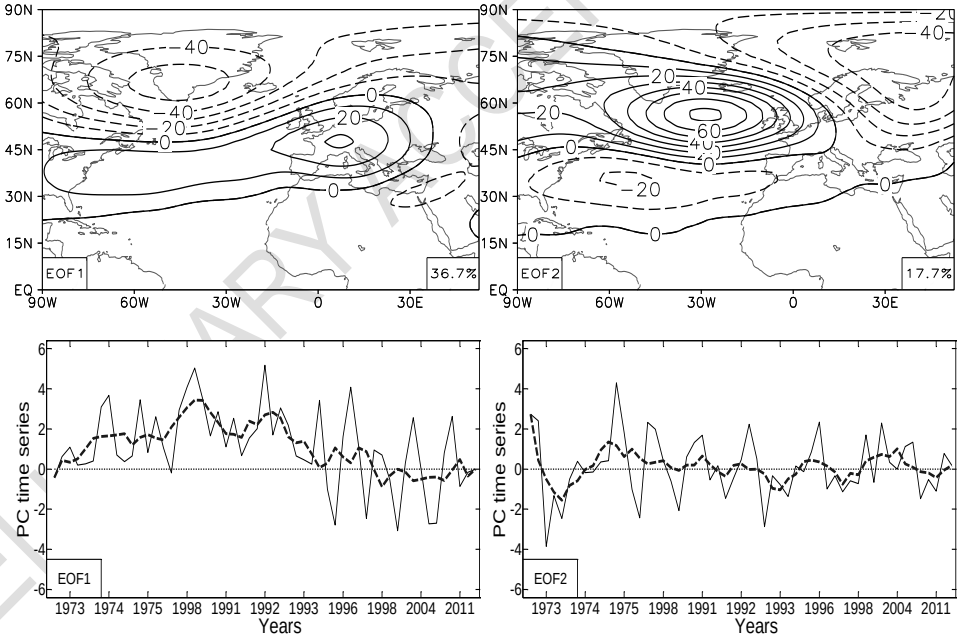

Fig. 3. Leading and second EOF components of monthly (November--March) mean geopotential height fields (units: m; contour interval: 10) at 500 hPa for high IB frequencies winters over (a) Northern Europe and (b) Southern Europe, and the corresponding principal component time series. The thick dotted line represents a 5-point moving average.

(a)

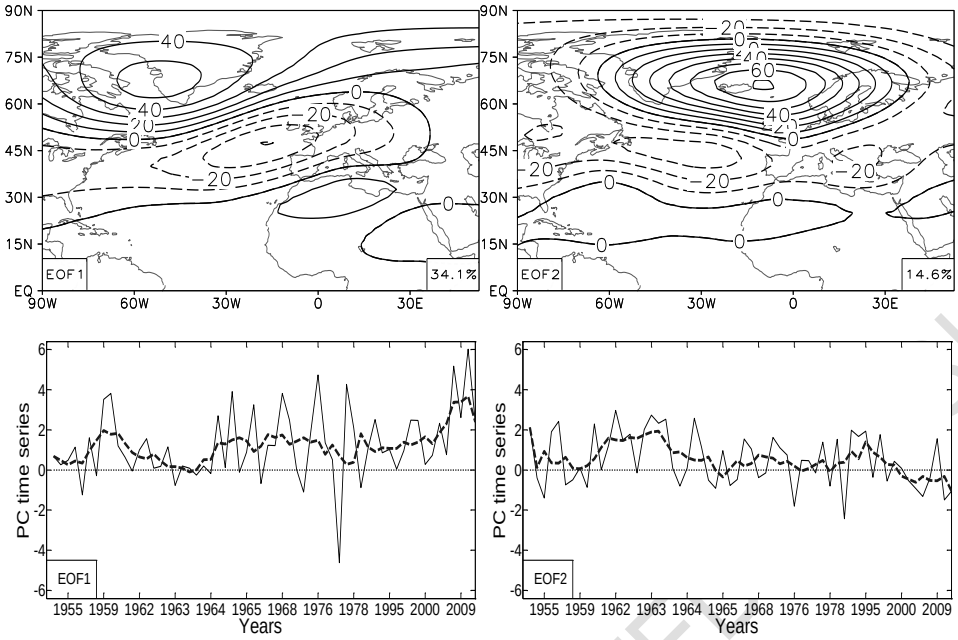

(b)

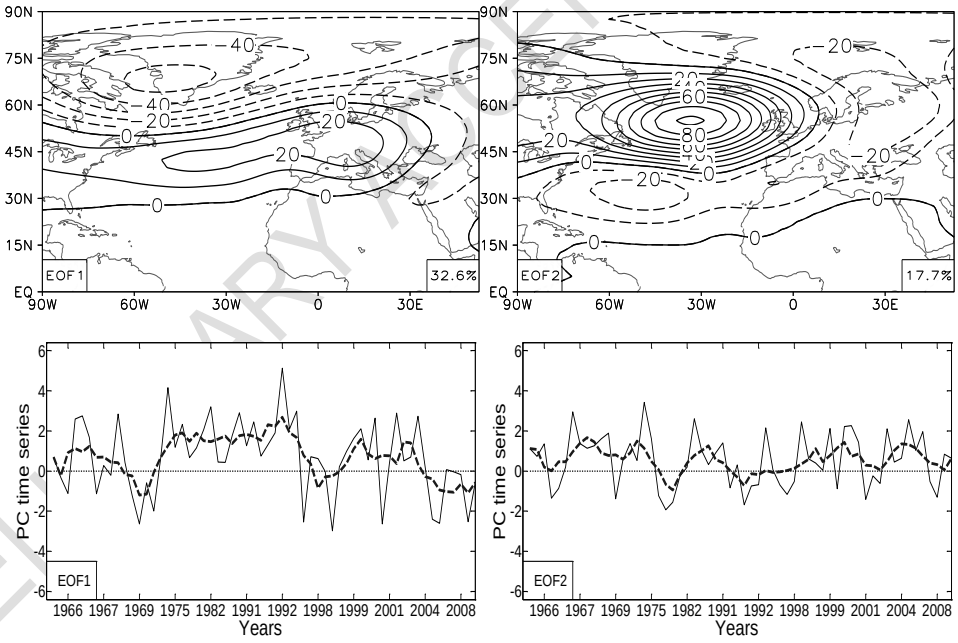

Fig. 4. As in Fig. 3, but for the (a) high-latitude North Atlantic and (b) low-latitude North Atlantic.

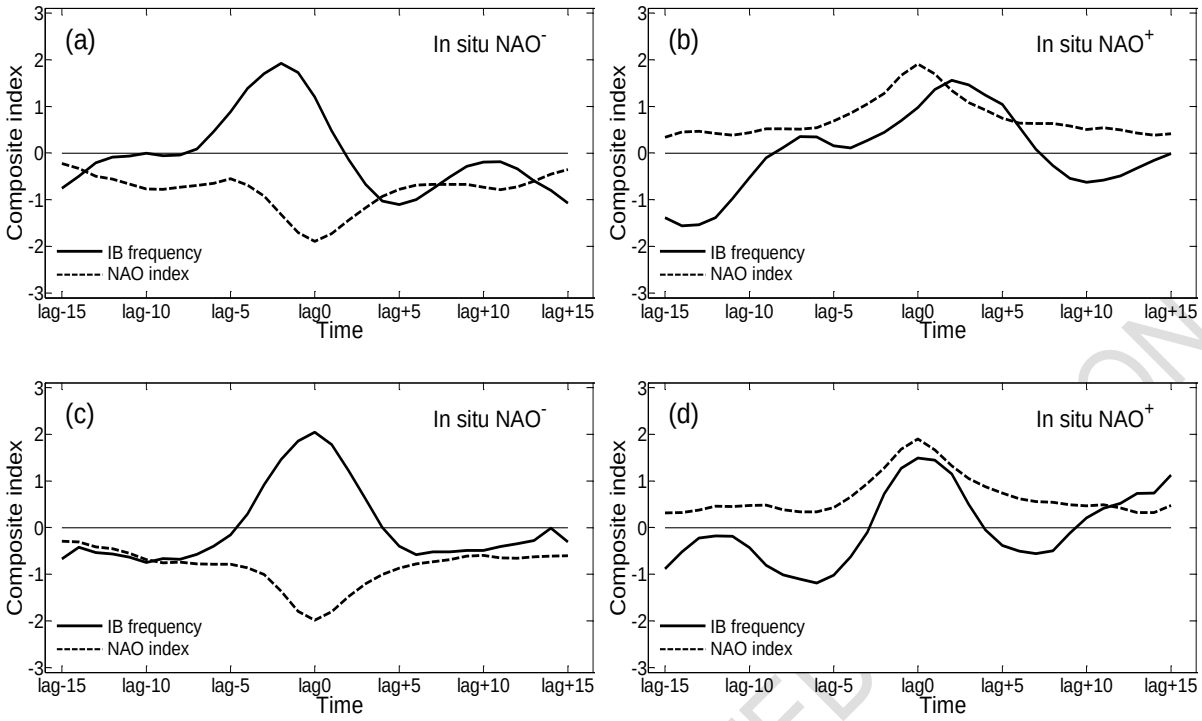

Fig. 5. Time series of normalized composite NAO index and IB frequency of high IB frequency winters averaged over different regions: (a) Northern Europe; (b) Southern Europe; (c) the high-latitude North Atlantic; and (d) the low-latitude North Atlantic. The correlation coefficients between IB frequency and NAO index time series are calculated during the period from lag(−10) to lag(+10).

(a)

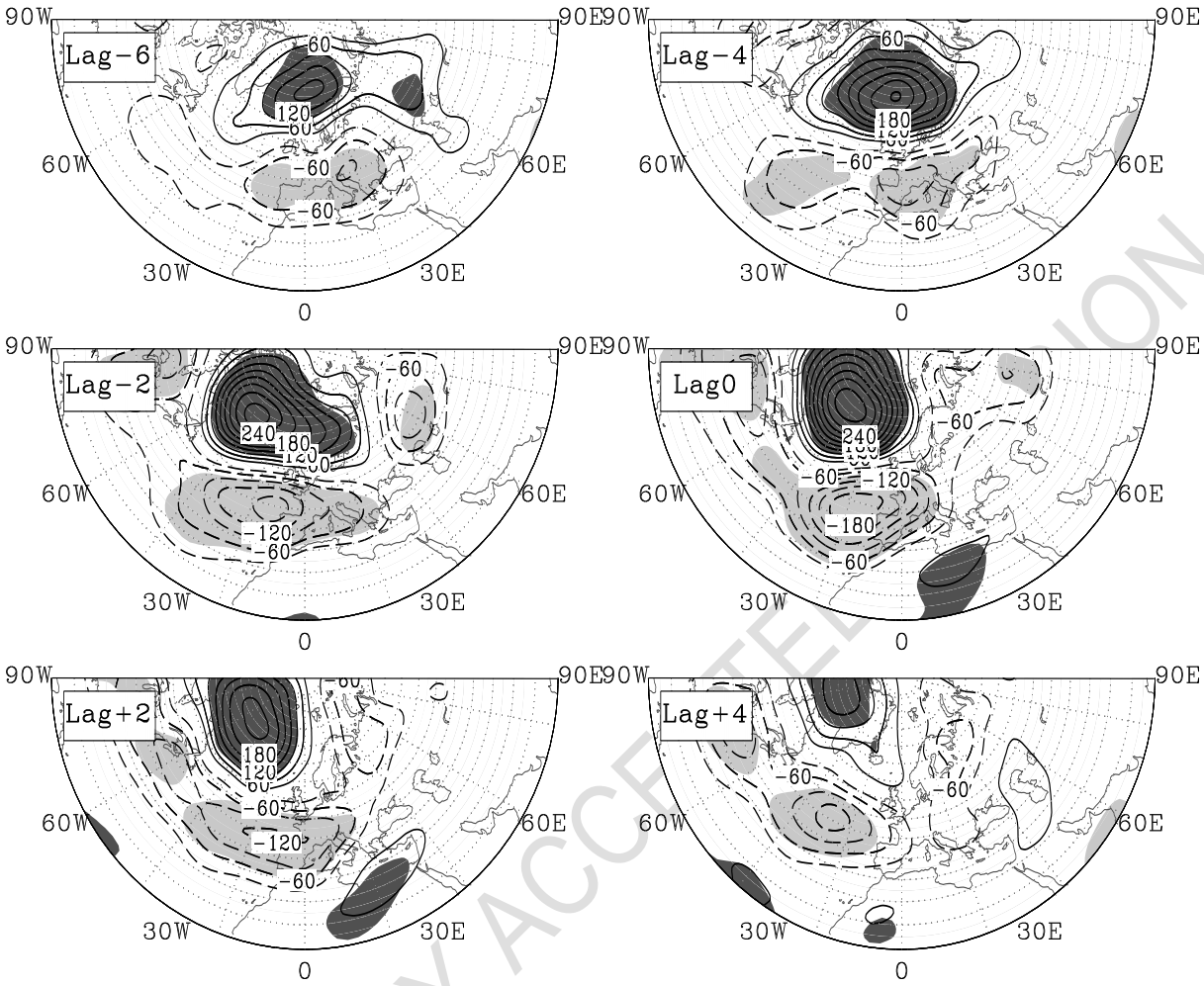

(b)

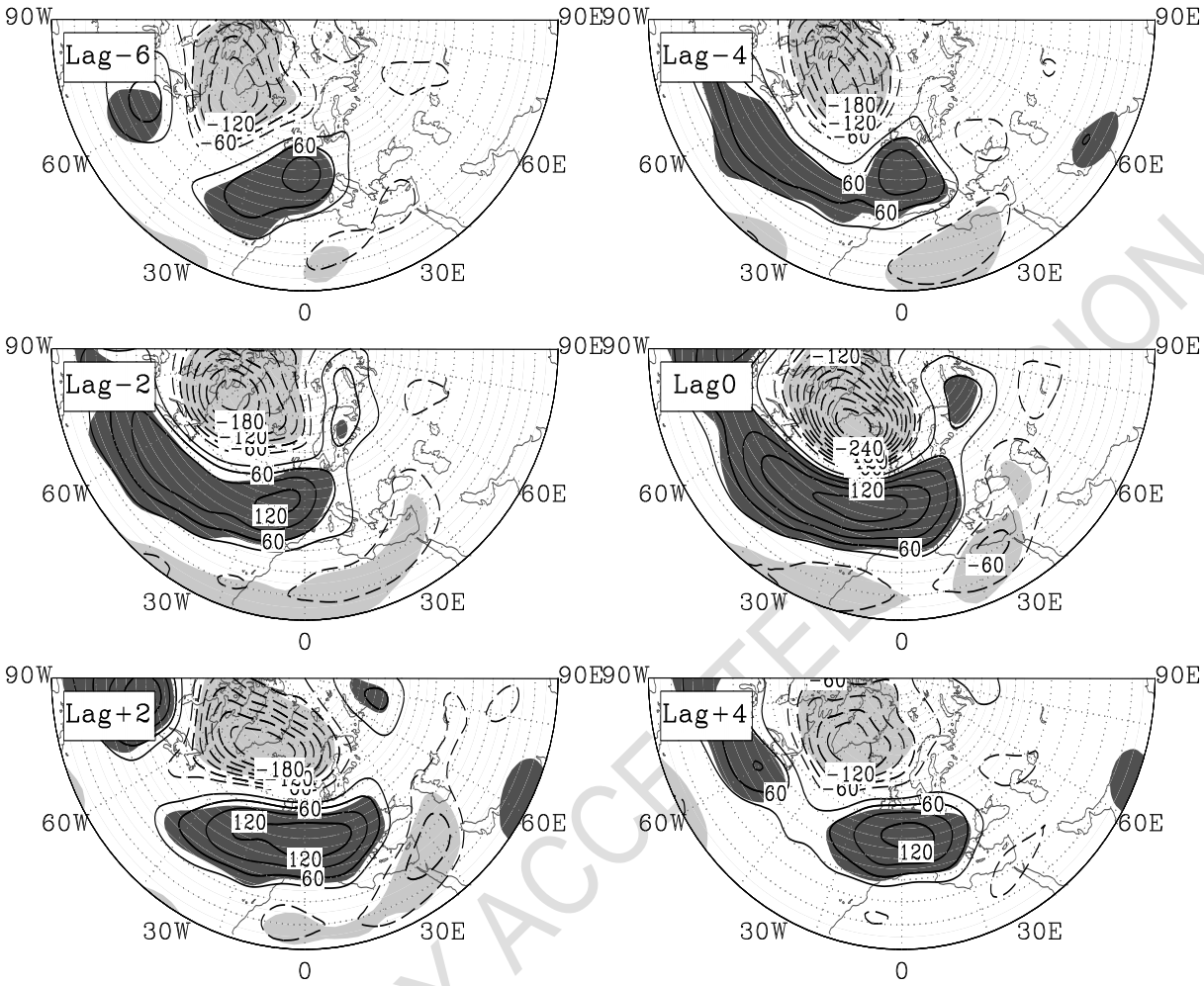

Fig. 6. Composite of daily 500-hPa geopotential height anomalies of (a) *in-situ* NAO^{-} events during high IB frequency winters over Northern Europe and (b) *in-situ* NAO^{+} events during high IB frequency winters over Southern Europe. The composites are applied from lag(−6) to lag(+4) in 2-day intervals for *in-situ* NAO events, in which lag(0) represents the day with maximum amplitude during the NAO life cycle. Contours are drawn with intervals of 30. The shading denotes regions above the 95% confidence level according to the two-sided Student's *t*-test. The lines of latitude are plotted in 5 °intervals starting at 20 ℃N. Units: m.

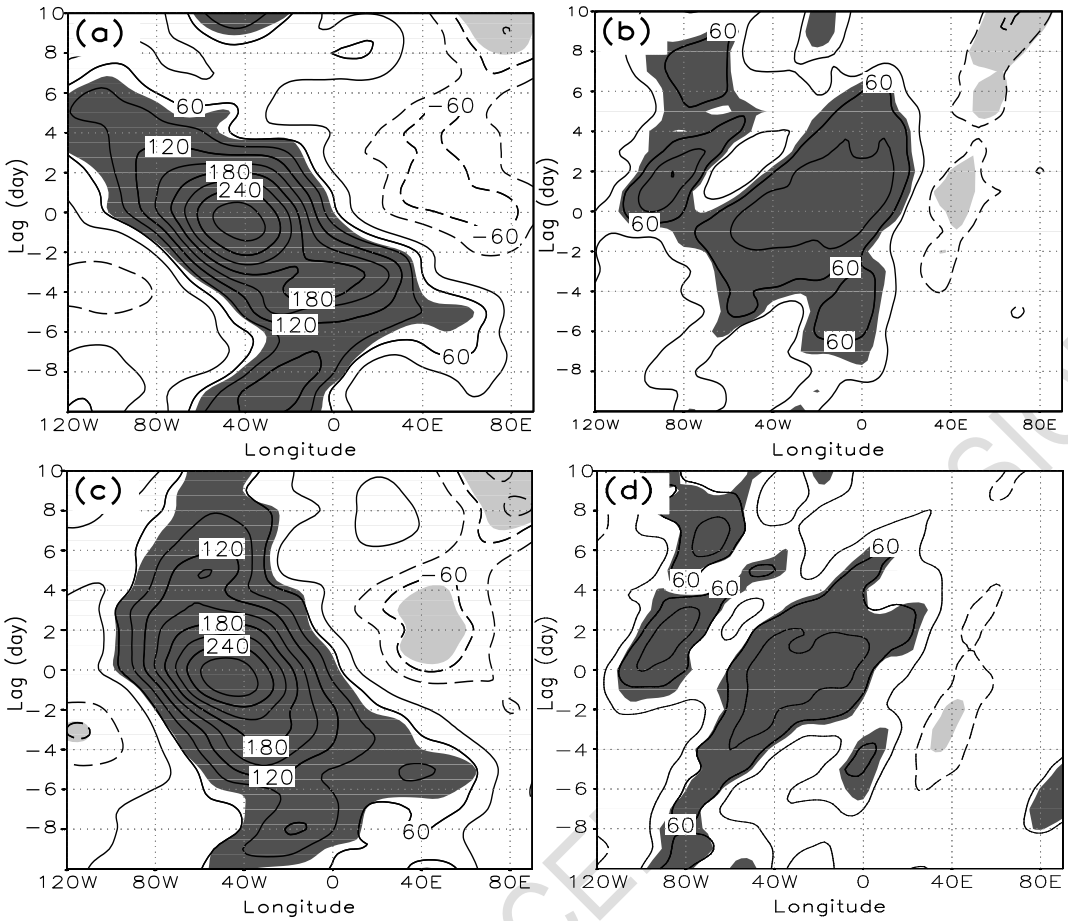

Fig. 7. Hovmöller diagrams of the composite daily geopotential height anomalies averaged over 60°–77.5°N (35°–50°N) for *in-situ* NAO^- (NAO^+) events. Composites of *in-situ* NAO^- events are shown in (a) and (c), while composites of *in-situ* NAO^+ events are displayed in (b) and (d). *In-situ* NAO^- events in (a) [(c)] are selected in high IB frequency winter years over Northern Europe [the high-latitude North Atlantic]. *In-situ* NAO^+ events in (b) [(d)] are selected in high IB frequency winter years over Southern Europe [the low-latitude North Atlantic]. Dark (light) shading indicates regions for positive (negative) geopotential height anomalies that above the 99% confidence level. Units: m.

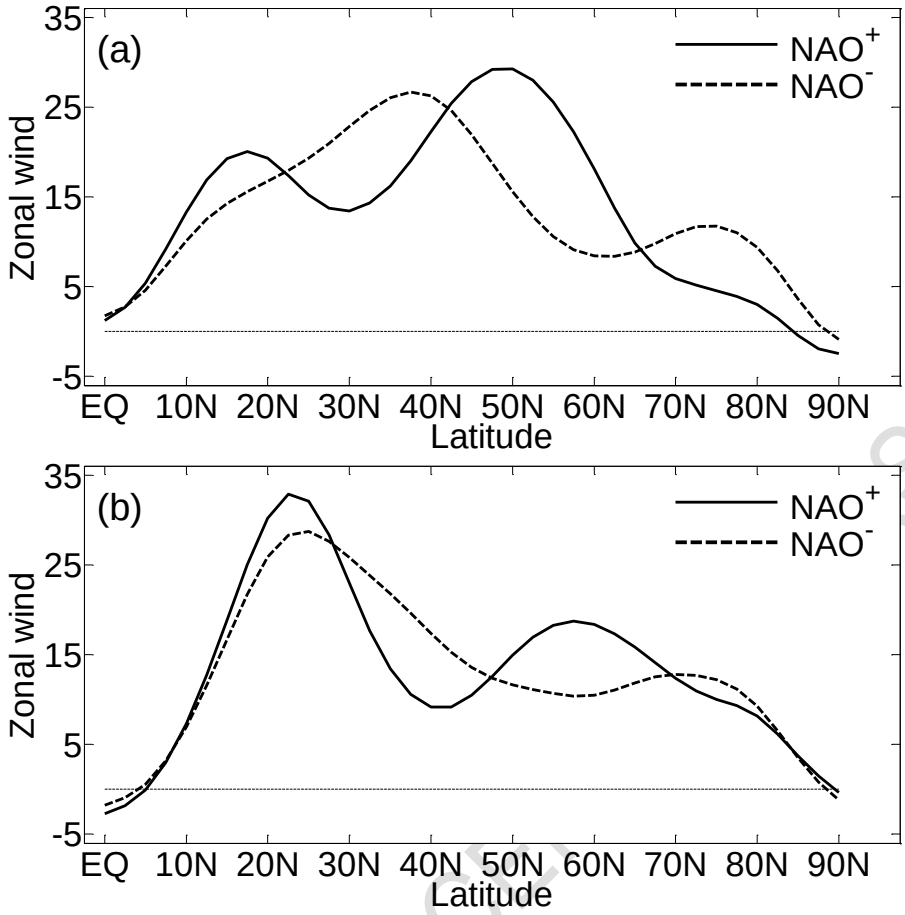

Fig. 8. Latitudinal distribution of time-mean zonal winds from lag(−10) to lag(+10) averaged over (a) the Atlantic basin (60 °--10 °W) and (b) continental Europe (10 °W--30 °E) during the life cycles of *in-situ* NAO^{-} and NAO^{+} events. Units: m s^{-1}.